Zhu *et al. Journal of Orthopaedic Surgery and Research (2025) 20:96*
https://doi.org/10.1186/s13018-025-05500-0

Journal of Orthopaedic Surgery and Research

RESEARCH **Open Access**

Exploring the optimal reconstruction strategy for Enneking III defects in pelvis bone tumors: a finite element analysis

Jiazhuang Zhu[1,2†], Jianping Hu[1,2†], Kunpeng Zhu[1,2], Xiaolong Ma[1,2], Zhen Huang[1,2] and Chunlin Zhang[1,2*]

Abstract

Background Controversy exists regarding the reconstruction of bone defects in Enneking III. This study aimed to use the finite element analysis (FEA) method to clarify (1) the utility of reconstructing the pelvis Enneking III region and (2) the optimal approach for this reconstruction.

Methods FEA models were generated for three types of Enneking III defects in the pelvis, replacing all the defect areas in region III with a sizable solid box for topology optimization (TO). Based on the defect location and TO results, three reconstruction schemes were designed for each type of defect. We subsequently conducted simulations of static FEA under natural walking loads using ANSYS software (version 2022R1, Canonsburg, Pennsylvania, USA).

Results Compared with Scheme A, reconstruction of the Enneking III region (Schemes B and C) led to a more uniform stress distribution and lower peak stress in the pelvis. Moreover, prostheses and screws exhibit decreased peak stress and deformation, with complex reconstruction schemes (C) outperforming simpler ones (B).

Conclusions The FEA results suggest that reconstructing Enneking Zone III defects improves stress distribution and reduces peak stress in the pelvis compared to non-reconstruction, potentially enhancing stability and reducing fracture risks. Complex reconstruction schemes involving more contralateral pelvis regions demonstrate superior biomechanical performance. However, clinical decisions should be individualized, integrating biomechanical insights with comprehensive patient-specific factors.

Keywords Pelvis bone tumors, Enneking III defects, Optimal reconstruction strategy, Finite element analysis, Topology optimization

Introduction

Managing pelvis tumors presents a formidable challenge for orthopedic oncologists. Several pelvis reconstruction methods, such as allografts, autografts [1–3], hip transposition [4], and prosthetic reconstruction [5–16], are available. Prosthetic reconstruction has recently gained popularity because of its high stability, relatively few complications, aesthetic benefits, and early weight-bearing capacity. However, controversy exists reconstruction for Enneking III defects in the pelvis [17, 18].

To maintain weight-bearing continuity and avoid complications such as fractures and nonunion, region III reconstruction is typically avoided [19, 20]. However,

[†]Jiazhuang Zhu and Jianping Hu have contributed equally to this manuscript.

*Correspondence:
Chunlin Zhang
shzhangchunlin123@163.com
[1] Department of Orthopedic Surgery, Shanghai Tenth People's Hospital, Tongji University School of Medicine, 301 Yanchang Middle Road, Shanghai 200072, People's Republic of China
[2] Institute of Bone Tumor Affiliated to Tongji University School of Medicine, Shanghai, People's Republic of China

complications can arise from not reconstructing region III, with postoperative hernias being the most common [21, 22]. Therefore, some studies advocate that bone reconstruction enhances functionality and reduces complications, supporting the use of mesh and soft tissue fixation [12, 17, 18, 23]. However, research reports a higher infection rate, prosthesis fractures, and an increased risk of pubic symphysis deformation after region III bone reconstruction [5, 17, 24–27]. Overall, further research is needed to determine whether bone reconstruction for region III defects is advisable.

We were unable to identify studies that have used the FEA method to explore the utility of reconstructing the pelvis Enneking III region. FEA divides a complex structure into finite elements and elucidates mechanical behavior using element-based calculations. FEA is widely used in mechanical stress and failure analysis and has frequently been applied to the pelvic region [28–31]. Therefore, FEA is a powerful tool for exploring the biomechanical characteristics of pelvis prosthetic reconstruction.

We used the FEA method to examine the stress and deformation levels of three Enneking III reconstruction schemes—the Enneking I + II + III, II + III, and isolated III regions—during normal walking. The purposes were to clarify (1) the utility of reconstructing the pelvis Enneking III region and (2) the optimal approach for this reconstruction.

Methods

We obtained three CT datasets of patients with pelvis tumors from our hospital's image database and constructed FEA models for three types of pelvis bone defects. Type 1 represents Enneking I + II + III, involving defects of the ilium, acetabulum, ischium, and pubis. Type 2 corresponds to Enneking II + III, with defects of the acetabulum, ischium, and pubis. Type 3 represents Enneking III, involving defects exclusively in the ischium and pubis. For Types 1 and 2 defects, we initially designed prosthetic reconstruction schemes excluding region III defects, whereas Type 3 defects remained unreconstructed. We then followed the method of Iqbal et al. [32], replacing all region III areas with a sizable solid box and performing a topology optimization (TO) to identify the optimal reconstruction method for region III (Fig. 1A–C). Based on the defect location, TO results, and our clinical experience, we developed three reconstruction options for each type (Fig. 1D–L). Scheme A involves no reconstruction of region III. Scheme B is a relatively simple reconstruction, involving fewer or no contralateral pelvis regions. Scheme C is a more complex reconstruction, involving more contralateral pelvis regions.

Following a previously reported protocol [16], three-dimensional (3D) pelvis models were constructed on the basis of DICOM-formatted CT data using Mimics software (version 21.0, Materialise, Leuven, Belgium). The pelvis-prosthesis FEA models were then built using Geomagic Wrap software (version 2017, USA), SOLIDWORKS software (version 2021, Dassault Systemes, France), and HyperMesh software (version 2022, Altair Engineering Inc, USA). A mesh sensitivity analysis of the pelvis FEA model revealed that a mesh size less than 1 mm limits the impact on the FEA results to less than 5%. Therefore, the mesh size of the pelvis-prosthesis model was set uniformly to 1 mm.

Next, we will assign material properties to the pelvis. Previous studies have shown that bone material properties can be categorized as homogeneous or inhomogeneous, with the former reducing FEA complexity but potentially yielding less accurate results [33, 34]. Therefore, we chose inhomogeneous material properties, which are more complex but improve FEA accuracy [34, 35]. Inhomogeneous bone material properties are assigned in the Mimics software on the basis of the corresponding gray-value using Eqs. (1) and (2) [32, 36]. Finally, the model was imported into ANSYS software (version 2022R1, Canonsburg, Pennsylvania, USA), where other material properties were assigned, and FEA and TO were conducted. The material properties of each part of the model are detailed in Table 1 [32, 36, 37].

The load magnitude and direction presented in Table 2 simulate the most common of the six main human activities: pelvis loading during normal walking (data referenced from Iqbal et al. [32]). A full constraint was applied to the superior surface of the sacrum. All contacts in the FEA model were defined as bonded to simulate the force conditions following osteointegration of the prosthesis and host bone, which typically occurs at least 6 months postoperatively [38, 39]. The biomechanical characteristics of each reconstruction scheme were evaluated by assessing the peak stress, stress distribution, and deformation of the pelvis, prosthesis, screws (excluding region III), and region III.

$$\rho = 6.9141e^{-4} \times HU + 1.026716 \tag{1}$$

$$E = 2017.3 \times \rho^{2.46} \tag{2}$$

Results

TO results are presented in Fig. 2. For Types 1 and 2 defects, the TO results are hollow, making reconstruction challenging; thus, we developed reconstruction schemes on the basis of experience. In Scheme B, one screw is used to anchor the prosthesis to the contralateral pubis.

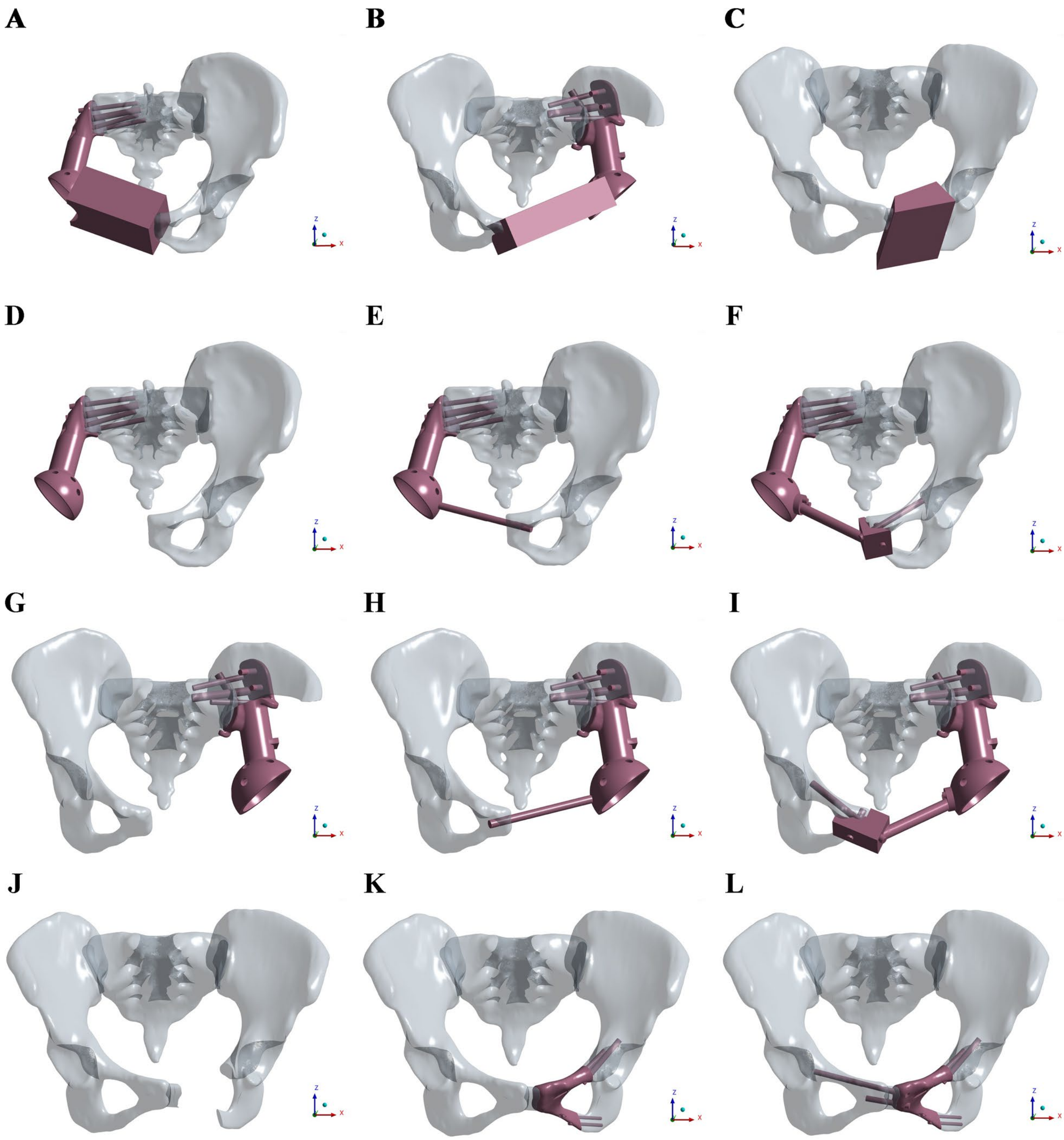

Fig. 1 Reconstruction schemes for sizable solid boxes and Types 1–3. **A–C** Solid boxes for Types 1 to 3; **D–F** Reconstruction schemes for Type 1A-C, each including three S1 screws and one S2 screw, with Type 1B adding one screw to secure the prosthesis to the contralateral pubis, and Type 1C replaces the screws of Type 1B with a pubic plate and adds one contralateral anterior acetabular column screw and one contralateral pubic screw; **G–I** Reconstruction schemes for Type 2A-C, each including three screws passing only through the remaining ilium and three S1 screws, with Type 2B adding one screw to anchor the prosthesis to the contralateral pubis, and Type 2C replaces the screws of Type 2B with a pubic plate and adds one contralateral anterior acetabular column screw and one contralateral pubic screw; **J–L** Reconstruction schemes for Type 3A-C, where Type 3B and 3C both include two anterior acetabular column screws and two ischium screws, with Type 3C further adding one contralateral anterior column screw and one contralateral pubis screw

Table 1 Material properties of the entities

Entity	Material	Elastic modulus (MPa)	Poisson's ratio
Pelvis	Inhomogeneous		0.3
Sacroiliac joint	Homogeneous	54	0.4
Symphysis pubis	Homogeneous	5	0.45
Prostheses	Ti–6Al–4V	110,000	0.3
Screws	Ti–6Al–4V	110,000	0.3
Sizable solid box	Ti–6Al–4V	110,000	0.3

Table 2 Force of the pelvis during normal walking

Application side	F_x(N)	F_y(N)	F_z(N)	Combined forces(N)
Affected acetabulum	±230.18 (Right: +, Left: −)	− 164.39	1495.24	1521.8
Contralateral acetabulum	±325.45 (Left: −, Right: +)	− 39.26	446.75	554.12

In Scheme C, the screws in Scheme B are replaced with a pubic plate, and one contralateral anterior acetabular column screw and one contralateral pubic screw are added. However, for Type 3 defects, the TO result resembles the original shape of the ischium and pubis, so we designed reconstruction prostheses on the basis of the original shape. Additionally, Schemes B and C both include two anterior acetabular column screws and two ischium screws, with Scheme C further adding one contralateral anterior acetabular column screw and one contralateral pubis screw.

Type 1 defects

Figure 3 and Table 3 present the FEA results for Type 1 defects. Scheme C demonstrates a more uniform stress distribution for the pelvis with a significant reduction in peak stress compared with both Schemes A and B (Fig. 3A–C). However, pelvis deformation increases in Scheme C (Fig. 3D–F). For the prosthesis (Fig. 3G–L), Scheme C results in the lowest stress and deformation levels. With respect to the screws (excluding region III) (Fig. 3M–R), Scheme C reduces both the stress and deformation compared with those of Schemes A and B. In Region III (Fig. 3S, T), Scheme C has a higher stress but significantly lower deformation compared to Scheme B (Fig. 3U, V).

Type 2 defects

Figure 4 and Table 4 present the FEA results for Type 2. Compared with both Schemes A and B, Scheme C results in a reduction in the peak stress of the pelvis (Fig. 4A–C); however, the degree of pelvis deformation is slightly

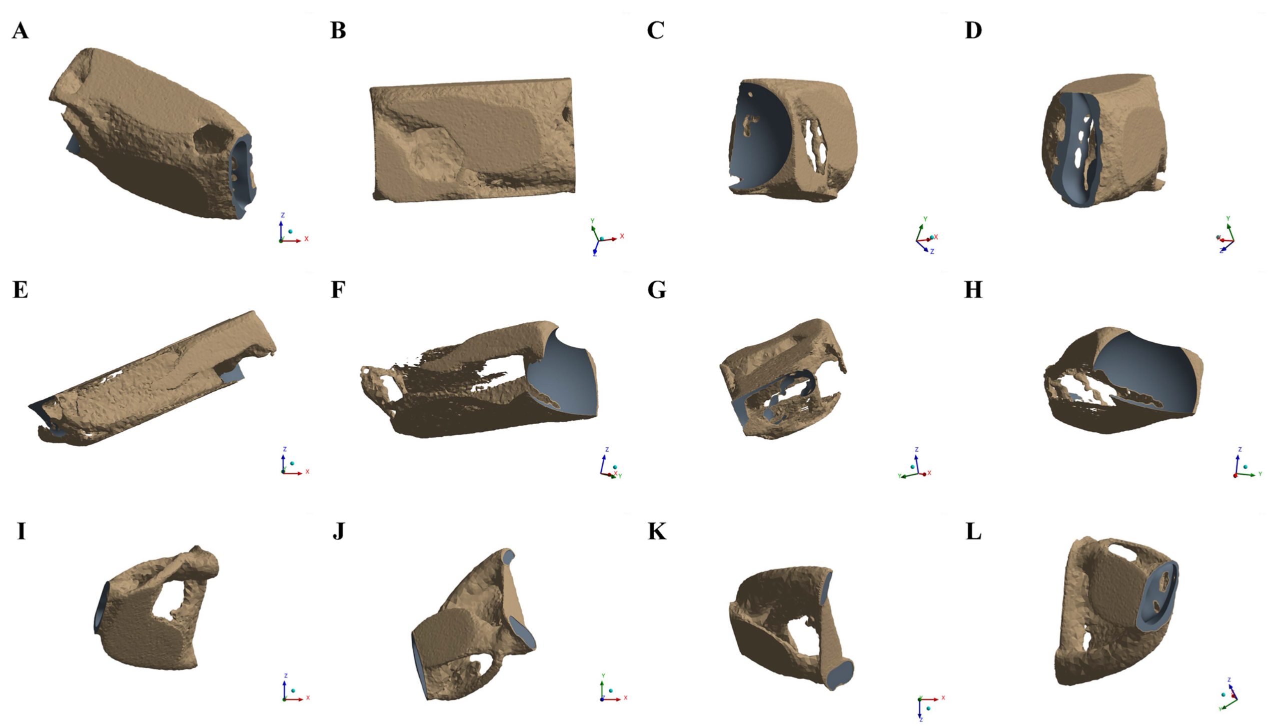

Fig. 2 TO results. **A–D** Type 1 defects; **E–H** Type 2 defects; **I–L** Type 3 defects

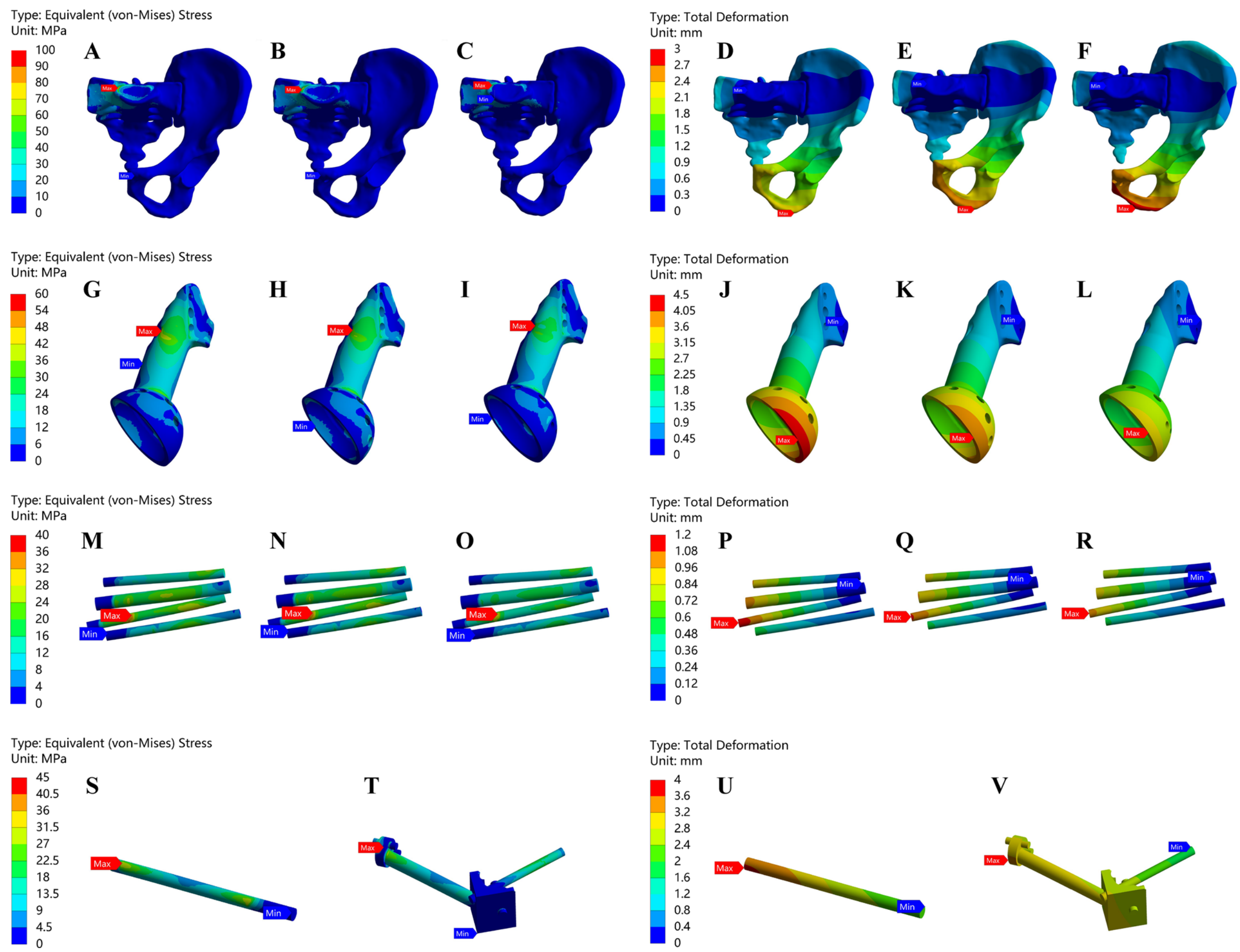

Fig. 3 FEA results for three reconstruction schemes for Type 1 defects. **A**–**C** Pelvis stress distribution for Type 1A-C; **D–F** Pelvis deformation for Type 1A-C; **G–I** Prosthesis stress distribution for Type 1A-C; **J–L** Prosthesis deformation for Type 1A-C; **M–O** Screws (excluding region III) stress distribution for Type 1A-C; **P–R** Screws (excluding region III) deformation for Type 1A-C; **S**, **T** Region III stress distribution for Type 1B-C; (**U-V)** Region III deformation for Type 1B-C

Table 3 Peak stresses and total deformation in the pelvis, prosthesis, screws (except region III) and region III for Type 1 defects

Type 1 defects	**A**	**B**	**C**
Peak stress (MPa)			
Pelvis	90.081	89.827	56.414
Prosthesis	55.319	53.318	44.354
Screws (except region III)	36.117	34.988	32.876
Region III	/	31.95	41.753
Total deformation (mm)			
Pelvis	2.2499	2.6128	2.8153
Prosthesis	4.3698	4.0026	3.3796
Screws (except region III)	1.1805	1.1011	1.0177
Region III	/	3.6436	3.2249

greater than that in Scheme B (Fig. 4D–F). For the prosthesis (Fig. 4G–L), Scheme C results in the lowest stress and deformation values. In terms of screws (excluding region III) (Fig. 4M–R), Scheme C achieves notable stress reduction compared with Schemes A and B, with minimal differences in deformation. In region III (Fig. 4S, T), Scheme C results in significantly greater stress and deformation compared to Scheme B (Fig. 4U, V).

Type 3 defects

Figure 5 and Table 5 show the FEA results for Type 3 defects. Schemes B and C show lower stress levels near the affected sacroiliac joint compared to Scheme A, with Scheme C achieving the most uniform stress distribution and the lowest deformation (Fig. 5A–F). For the prosthesis (Fig. 5G–J), although Scheme C results in a higher peak stress than Scheme B does, it results in a

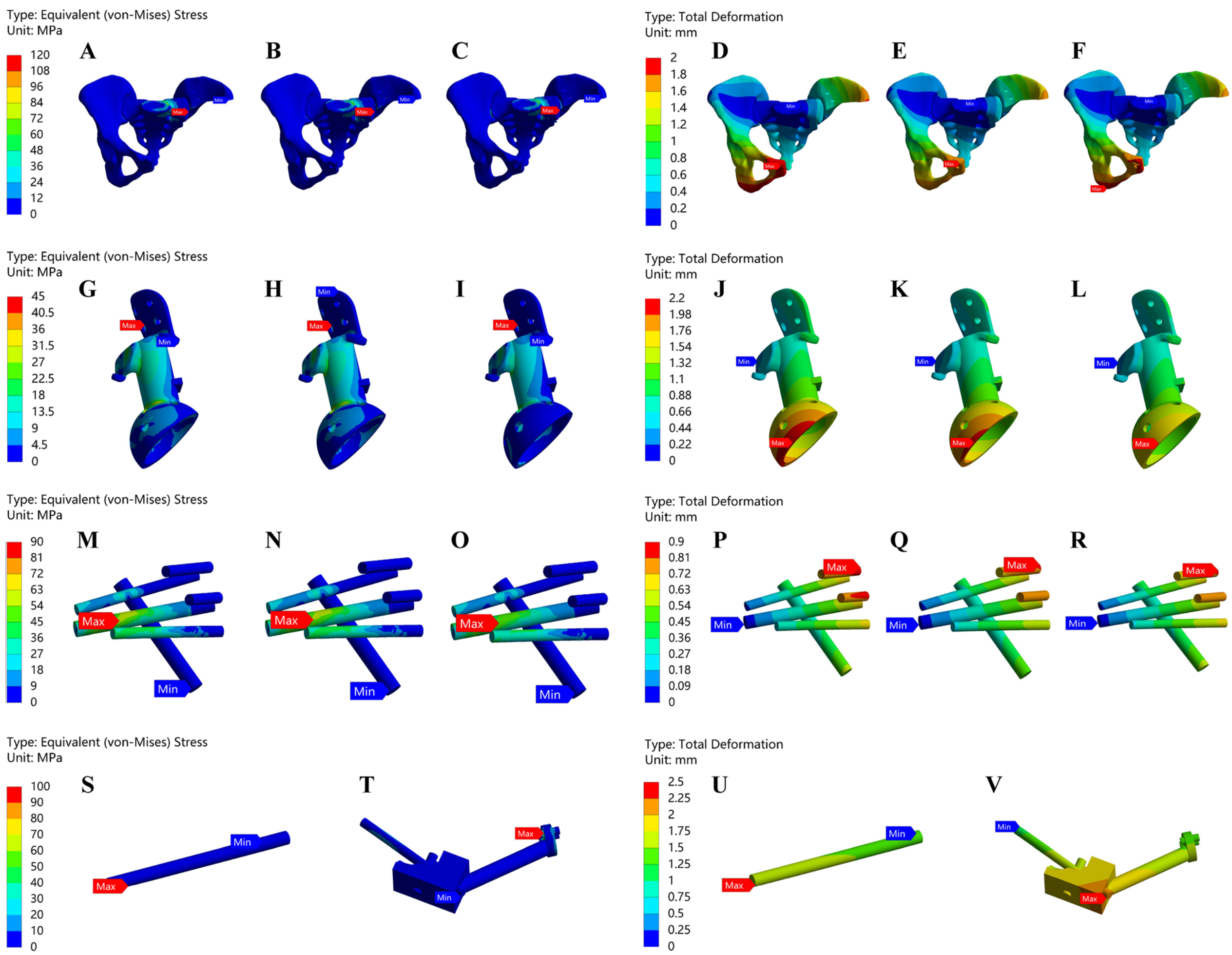

Fig. 4 FEA results for three Type 2 defects. **A**–**C** Pelvis stress distribution for Type 2A-C; **D–F** Pelvis deformation for Type 2A-C; **G–I** Prosthesis stress distribution for Type 2A-C; **J–L** Prosthesis deformation for Type 2A-C; **M–O** Screws (excluding region III) stress distribution for Type 2A-C; **P–R** Screws (excluding region III) deformation for Type 2A-C; **S**, **T** Region III stress distribution for Type 2B-C; **U**, **V** Region III deformation for Type 2B-C

more uniform stress distribution and reduced deformation. With respect to the screws (Fig. 5K–N), Scheme C reduces both the stress and deformation compared with Scheme B.

Table 4 Peak stresses and total deformation in the pelvis, prosthesis, screws (except region III) and region III for Type 2 defects

Type 2 defects	A	B	C
Peak stress (MPa)			
Pelvis	114.49	106.63	98.31
Prosthesis	40.447	38.168	36.352
Screws (except region III)	83.878	83.219	73.763
Region III	/	2.7112	96.808
Total deformation (mm)			
Pelvis	1.9963	1.7893	1.9303
Prosthesis	2.1445	2.0493	1.7088
Screws (except region III)	0.86411	0.82262	0.83051
Region III	/	1.7521	2.1435

Discussion

This study used FEA and TO methods to develop reconstruction schemes for three types of Enneking III defects in the pelvis. For each type of defect, three reconstruction schemes were proposed: non-reconstruction (Scheme A), simple reconstruction (Scheme B), and complex reconstruction (Scheme C). This study aimed to biomechanically assess the utility of reconstructing Enneking III defects in bone tumors and identify the optimal reconstruction strategy. The FEA results show that both Schemes B and C generally outperform Scheme A biomechanically, achieving a more uniform stress distribution and lower peak stresses in the pelvis, as well as

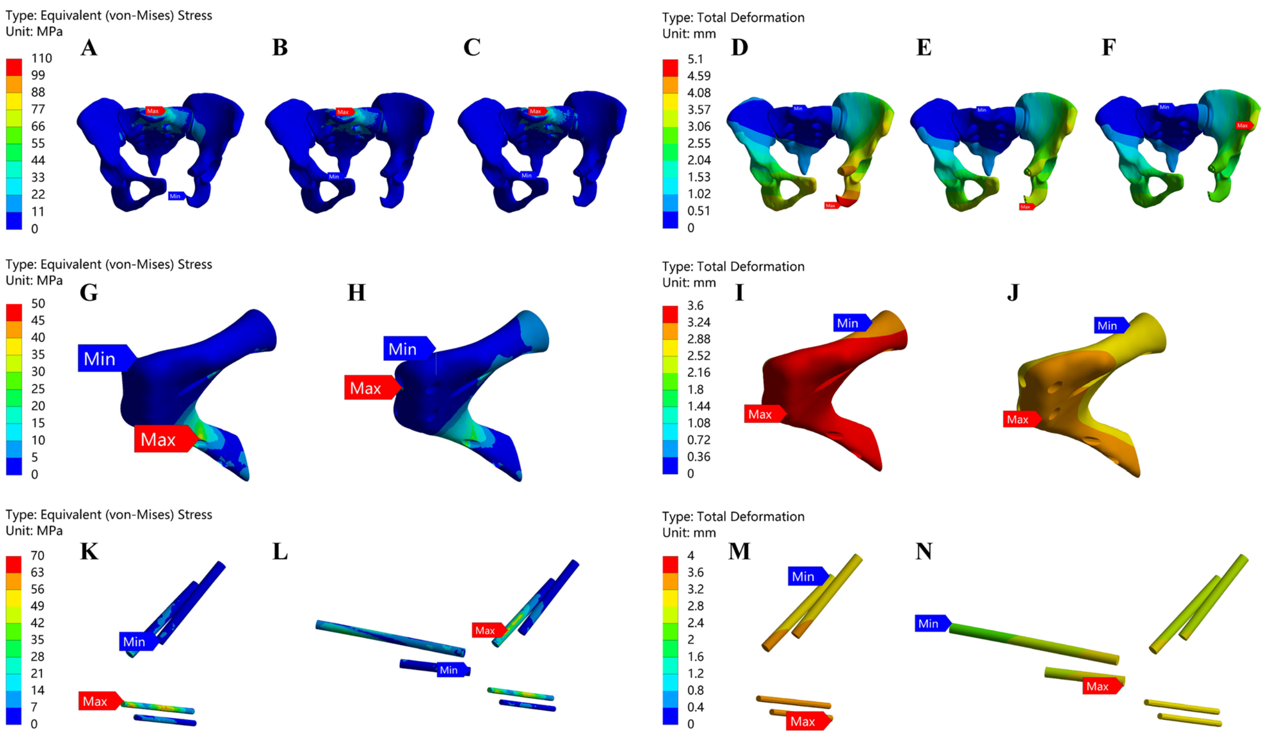

Fig. 5 FEA results for three reconstruction schemes for Type 3 defects. **A**–**C** Pelvis stress distributions for Type 3A-C; **D–F** Pelvis deformation for Type 3A-C; **G–H** Prosthesis stress distributions for Type 3B-C; **I–J** Prosthesis deformation for Type 3B-C; **K–L** Screws stress distributions for Type 3B-C; **M–N** Screws deformation for Type 3B-C

Table 5 Peak stresses and total deformation in the pelvis, prosthesis, and screws for Type 3 defects

Type 3 defects	A	B	C
Peak stress (MPa)			
Pelvis	97.305	101.74	97.199
Prosthesis	/	37.413	48.476
Screws	/	66.829	61.106
Total deformation (mm)			
Pelvis	5.0835	3.6374	3.2738
Prosthesis	/	3.576	3.0293
Screws	/	3.5409	3.0537

reduced peak stresses and deformations in the prostheses and screws, with complex reconstruction performing better than simple reconstruction. This reduces the risk of stress fractures and prosthesis fractures.

Reducing peak stress and achieving uniform stress distribution are crucial for reconstructing pelvis bone defects with prosthetics. This helps prevent pathological fractures and breakage of prostheses or screws, thereby enhancing the long-term stability of the prosthesis[32, 40, 41]. The FEA results show that the pelvis stress is concentrated at the fixed edge of S1 on the side with greater force. In Types 1 and 2 pelvis defects involving the acetabulum, stress levels in the pelvis, prosthesis, and screws (excluding region III) are lower in both reconstruction schemes than in the Scheme A, with Scheme C outperforming Scheme B. Additionally, stress in the defect area (region III) is concentrated at the connection with the artificial acetabulum. For Type 3 defects, which involve only a defect in the ischium and pubis, Scheme C is lower than Scheme B in terms of the prosthesis peak stress but higher in terms of the peak stress of the screw. However, the stress levels in the pelvis bone are similar for both reconstruction schemes. Most importantly, for all three types, the peak stress in the pelvis bone under Scheme C is lower than the yield strength of the cortical bone (150 MPa) [42]. Additionally, the peak stress in the prosthesis and screws is significantly lower than the yield strength (789–1013 MPa) and fatigue limit (310–610 MPa) of Ti–6Al–4V [43, 44]. As a result, reconstructing region III reduces the risk of complications such as prosthesis and screw loosening and breakage, with complex reconstruction outperforming simple reconstruction.

Deformation of the pelvis and prosthesis is a key indicator for assessing reconstruction stability. Smaller deformation indicates less local stress concentration and improved reconstruction stability [14, 41, 45–47]. For Types 1 and 2 defects, first, the maximum total deformation of the pelvis is near the intact obturator foramen, and the maximum total deformation of the prosthesis is at the edge of the artificial acetabulum. Second, for total pelvis deformation, both Schemes B and C for Type 1 defects result in greater deformations than the Scheme A does, whereas the opposite is true for Type 2 defects. Third, for the prosthesis and screw deformation levels (excluding region III), both Schemes B and C for Types 1 and 2 defects are lower than the Scheme A. Furthermore, for Type 1 defects, Scheme C outperforms Scheme B. However, for Type 2 defects, the two reconstruction schemes are similar. For Type 3 defects, the maximum total deformation in the pelvis is near the affected side obturator foramen. Moreover, in terms of total deformation of the pelvis, prosthesis, and screws, both Schemes B and C are lower than in the Scheme A scenario, with Scheme C outperforming Scheme B. Overall, reconstructing region III effectively enhances the stability of bone defect reconstruction compared with non-reconstruction.

The pelvis is a closed ring structure formed by the sacroiliac joints and the pubic symphysis. The anterior ring, which includes the pubic symphysis, contributes 40% of the overall stability of the pelvis ring [26]. Moreover, loss of the pubic symphysis increases the load on the sacroiliac joints, leading to joint instability and osteoarthritis [48]. As a result, the integrity of the anterior ring is crucial for stress distribution in the pelvis. Growing research supports the construction of a complete pelvis ring [10, 12, 17, 18, 23, 49–53]. For example, Wang et al. [10] performed hemipelvic prosthesis reconstruction on 11 patients with periacetabular bone tumors, with an average follow-up time of 15.5 months. The results revealed an average MSTS-93 lower limb function score of 19.2. Wang et al. [50] designed pelvis ring reconstruction prostheses for 13 patients with periacetabular bone tumors and conducted short-term follow-up. The results revealed a median MSTS-93 score of 23, a median VAS score of 2, and successful bone integration for all prostheses. Zhang et al. [12] conducted an average 23.6-month follow-up for 5 patients who underwent Type 3 hemipelvic prosthesis reconstruction and reported an average MSTS score of 29.8, with bone integration observed in all patients. Jamshidi et al. [23] conducted a mean 6-year follow-up on 32 patients who underwent Type 3 hemipelvic resection (15 reconstructed, 17 unreconstructed). The results revealed significantly higher average MSTS scores in the reconstructed group than in the unreconstructed group (26 and 22.7, $P<0.001$), with lower average VAS scores postoperatively (2.1 and 4.2, $P=0.016$). These studies confirm that bone reconstruction in region III results in improved function and fewer complications. Moreover, reconstruction of region III also supports soft tissue reconstruction and can enhance the biomechanical stability of pelvis reconstruction by evenly distributing deformation and stress through the addition of pedicle screw systems [12, 15, 54].

However, some studies disagree with the reconstruction of defects in region III. First, Dong et al. [27] reported found that bone reconstruction, including that in region III, for Type I + IV bone defects results in significant vertical deformation at the pubic symphysis. Second, for Type I + II + III or II + III bone defects involving the acetabulum, reconstruction via a pubic plate or other methods may lead to stress concentration on the pubic plate, increasing the risk of fracture. Reconstruction also prolongs the surgical time, increasing the chances of infection and bleeding [5, 17, 24–26]. Third, according to our clinical experience, the presence of important blood vessels and nerves in region III makes these structures susceptible to injury during reconstruction, leading to complications such as bleeding, delayed wound healing, or sensory abnormalities.

Therefore, significant controversy remains regarding the utility of reconstructing region III. Encouragingly, this study revealed that reconstructing region III resulted in a more uniform distribution of pelvis stress and a more stable prosthesis from a biomechanical standpoint. This sheds light on the question of whether to reconstruct region III.

This study has several limitations. First, we applied only one type of load (normal walking) and did not assess outcomes under different daily activities and gait cycle loads. Although normal walking was used as a standard reference, future studies should include patient-specific conditions, such as fast gait and limping gait, to better reflect postoperative variability [55]. Second, to streamline calculations and obtain results efficiently, our FEA model simplifies the screws to cylinders. This simplification may influence the accuracy of stress and deformation results, particularly in regions where the interaction between screws and surrounding bone is critical. Additionally, the exclusion of muscles and ligaments may explain why the maximum deformation in the pelvic model occurs at the bottom of the ischium, rather than at the iliac wing, which is where maximum deformation is observed in FEA studies that include these structures [56, 57]. Third, this study assumed full bonding between the host bone and the implant to explore optimal conditions; however, future studies should simulate partial bonding scenarios to better reflect real-world conditions. Fourth, this study relied exclusively on numerical research through FEA and omitted mechanical compression and clinical experiments to validate the findings. Finally, a limitation of FEA is that it simplifies the model, often excluding key structures such as blood vessels and nerves. As a result, prosthesis deformation during FEA may conflict with these sensitive structures, potentially leading to complications such as necrosis or amputation in clinical applications. However, these anatomical structures can be incorporated into the prosthesis design and FEA in future research to achieve a more balanced outcome.

Conclusions

The FEA results suggest that reconstructing Enneking Zone III defects, regardless of defect type, results in a more uniform stress distribution and lower peak stress in the pelvis compared to non-reconstruction under simulated walking loads. Stress levels remain below the yield strength of cortical bone, while prostheses and screws experience reduced peak stress and deformation, potentially increasing biomechanical stability and reducing the risk of fractures. Complex reconstruction schemes involving more contralateral pelvis regions demonstrate superior biomechanical performance compared to simpler schemes. However, biomechanical advantages observed in FEA simulations do not fully account for real-world clinical complexities when performing reconstruction, such as prolonged operative times, vascular and nerve injuries, or risks of reconstruction failure. These factors, along with patient preferences and oncologic prognosis, must be carefully considered. Finally, while reconstruction may offer biomechanical benefits, clinical decisions should be individualized, balancing biomechanical insights with patient-specific factors.

Abbreviations

FEA Finite element analysis
TO Topology optimization
3D Three-dimensional

Acknowledgements

Not applicable.

Author contributions

All authors contributed to the study conception and design. The CT data were acquired by JZ, JH and CZ. The finite element analysis and topology optimization were performed by JZ, JH, KZ, XM and ZH, and the data analysis was performed by JZ and JH. The first draft of the manuscript was written by JZ. JH and CZ revised the draft of the manuscript. All authors read and approved the final manuscript.

Funding

This research was funded by Grant from National Natural Science Foundation of China (Nos. 82072963, 82103513, 82303898), Climbing Talents Program of Shanghai Tenth People's Hospital (2021SYPDRC021) and Clinical Research Program of Shanghai Tenth People's Hospital (YNCR2B002, YNCR2C012), Program for Research-oriented Physician of Shanghai Tenth People's Hospital (2023YJXYSC001) and the Fundamental Research Funds for the Central Universities (22120240277).

Availability of data and materials

Data and materials for this study are available from the corresponding author on reasonable request.

Declarations

Ethics approval and consent to participate

The acquisition of CT data from pelvis tumor patients for this study was approved by the Ethics Committee of Shanghai Tenth People's Hospital, affiliated with Tongji University (SHSY-IEC-5.0/22K14).

Consent for publication

Not applicable.

Competing interests

The authors declare that they have no competing interests or personal relationships that could have appeared to influence the work reported in this paper.

Received: 20 October 2024 Accepted: 14 January 2025
Published online: 24 January 2025

References

1. Matejovsky Z Jr, Matejovsky Z, Kofranek I. Massive allografts in tumour surgery. Int Orthop. 2006;30(6):478–83.
2. Biau DJ, Thévenin F, Dumaine V, Babinet A, Tomeno B, Anract P. Ipsilateral femoral autograft reconstruction after resection of a pelvic tumor. J Bone Joint Surg Am. 2009;91(1):142–51.
3. Wafa H, Grimer RJ, Jeys L, Abudu AT, Carter SR, Tillman RM. The use of extracorporeally irradiated autografts in pelvic reconstruction following tumour resection. Bone Joint J. 2014;96-b(10):1404–10.
4. Xu H, Li Y, Zhang Q, Hao L, Yu F, Niu X. Does adding femoral lengthening at the time of rotation hip transposition after periacetabular tumor resection allow for restoration of limb length and function? Interim results of a modified hip transposition procedure. Clin Orthop Relat Res. 2021;479(7):1521–30.
5. Guo W, Li D, Tang X, Yang Y, Ji T. Reconstruction with modular hemipelvic prostheses for periacetabular tumor. Clin Orthop Relat Res. 2007;461:180–8.
6. Tang X, Guo W, Ji T. Reconstruction with modular hemipelvic prosthesis for the resection of solitary periacetabular metastasis. Arch Orthop Trauma Surg. 2011;131(12):1609–15.
7. Jansen JA, van de Sande MA, Dijkstra PD. Poor long-term clinical results of saddle prosthesis after resection of periacetabular tumors. Clin Orthop Relat Res. 2013;471(1):324–31.
8. Liang H, Ji T, Zhang Y, Wang Y, Guo W. Reconstruction with 3D-printed pelvic endoprostheses after resection of a pelvic tumour. Bone Joint J. 2017;99-b(2):267–75.
9. Bus MP, Szafranski A, Sellevold S, Goryn T, Jutte PC, Bramer JA, et al. LUMiC(®) endoprosthetic reconstruction after periacetabular tumor resection: short-term results. Clin Orthop Relat Res. 2017;475(3):686–95.
10. Wang B, Hao Y, Pu F, Jiang W, Shao Z. Computer-aided designed, three dimensional-printed hemipelvic prosthesis for peri-acetabular malignant bone tumour. Int Orthop. 2018;42(3):687–94.
11. Ogura K, Susa M, Morioka H, Matsumine A, Ishii T, Hamada K, et al. Reconstruction using a constrained-type hip tumor prosthesis after resection of malignant periacetabular tumors: a study by the Japanese Musculoskeletal Oncology Group (JMOG). J Surg Oncol. 2018;117(7):1455–63.
12. Zhang Y, Min L, Lu M, Wang J, Wang Y, Luo Y, et al. Three-dimensional-printed customized prosthesis for pubic defect: clinical outcomes in 5 cases at a mean follow-up of 24 months. BMC Musculoskelet Disord. 2021;22(1):405.
13. Zhu D, Fu J, Wang L, Guo Z, Wang Z, Fan H. Reconstruction with customized, 3D-printed prosthesis after resection of periacetabular Ewing's sarcoma in children using "triradiate cartilage-based" surgical strategy: a technical note. J Orthop Translat. 2021;28:108–17.
14. Hu X, Lu M, He X, Li L, Lin J, Zhou Y, et al. Hip reconstruction using a customized intercalary prosthesis with the rhino horn-designed uncemented stem for ultrashort proximal femur segments following tumor resection: a combined biomechanical and clinical study. BMC Musculoskelet Disord. 2022;23(1):852.

15. Guo Z, Peng Y, Shen Q, Li J, He P, Yuan P, et al. Reconstruction with 3D-printed prostheses after type I + II + III internal hemipelvectomy: finite element analysis and preliminary outcomes. Front Bioeng Biotechnol. 2022;10:1036882.
16. Zhu J, Hu J, Zhu K, Ma X, Wang Y, Xu E, et al. Design of 3D-printed prostheses for reconstruction of periacetabular bone tumors using topology optimization. Front Bioeng Biotechnol. 2023;11:1289363.
17. Karim SM, Colman MW, Lozano-Calderón SA, Raskin KA, Schwab JH, Hornicek FJ. What are the functional results and complications from allograft reconstruction after partial hemipelvectomy of the pubis? Clin Orthop Relat Res. 2015;473(4):1442–8.
18. Chao AH, Neimanis SA, Chang DW, Lewis VO, Hanasono MM. Reconstruction after internal hemipelvectomy: outcomes and reconstructive algorithm. Ann Plast Surg. 2015;74(3):342–9.
19. Sherman CE, O'Connor MI, Sim FH. Survival, local recurrence, and function after pelvic limb salvage at 23 to 38 years of followup. Clin Orthop Relat Res. 2012;470(3):712–27.
20. Hu X, Lu M, Zhang Y, Li Z, Wang J, Wang Y, et al. Pelvic-girdle reconstruction with three-dimensional-printed endoprostheses after limb-salvage surgery for pelvic sarcomas: current landscape. Br J Surg. 2023;110(12):1712–22.
21. Arkoulis N, Savanis G, Simatos G, Zerbinis H, Nisiotis A. Incisional hernia of the urinary bladder following internal hemipelvectomy. Int J Surg Case Rep. 2012;3(7):316–8.
22. Hope WC, Ferro LC, Snyder JA, Procter LD, Salluzzo JL. Hemipelvectomy hernia: case series and literature review. Hernia. 2021;25(5):1159–67.
23. Jamshidi K, Zandrahimi F, Bagherifard A, Mohammadi F, Mirzaei A. Type III internal hemipelvectomy for primary bone tumours with and without allograft reconstruction: a comparison of outcomes. Bone Joint J. 2021;103-b(6):1155–9.
24. Mankin HJ, Hornicek FJ. Internal hemipelvectomy for the management of pelvic sarcomas. Surg Oncol Clin N Am. 2005;14(2):381–96.
25. Ji T, Guo W, Tang S, Li D. Nonlinear finite element analysis of the breakage in pubic connection plate after pelvic reconstruction with modular hemipelvic endoprosthesis. Zhongguo Zuzhi Gongcheng Yanjiu yu Linchuang Kangfu. 2010;14(35):6500–3.
26. Tile M. Pelvic ring fractures: should they be fixed? J Bone Joint Surg Br. 1988;70(1):1–12.
27. Dong Y, Hu H, Zhang CQ. Biomechanical study of modular hemipelvic endoprosthesis for Type I-IV defect of pelvic tumor. Chin J Cancer Res. 2014;26(4):431–6.
28. Hu P, Wu T, Wang HZ, Qi XZ, Yao J, Cheng XD, et al. Biomechanical comparison of three internal fixation techniques for stabilizing posterior pelvic ring disruption: a 3d finite element analysis. Orthop Surg. 2019;11(2):195–203.
29. Xu Z, Jiang Y, Mu W, Li W, Zhang G, Jiang S, et al. Electrophysiological, biomechanical, and finite element analysis study of sacral nerve injury caused by sacral fracture. Front Bioeng Biotechnol. 2022;10: 920991.
30. Ji T, Guo W, Tang XD, Yang Y. Reconstruction of type II+III pelvic resection with a modular hemipelvic endoprosthesis: a finite element analysis study. Orthop Surg. 2010;2(4):272–7.
31. Kitamura K, Fujii M, Ikemura S, Hamai S, Motomura G, Nakashima Y. Does patient-specific functional pelvic tilt affect joint contact pressure in hip dysplasia? A finite-element analysis study. Clin Orthop Relat Res. 2021;479(8):1712–24.
32. Iqbal T, Wang L, Li D, Dong E, Fan H, Fu J, et al. A general multi-objective topology optimization methodology developed for customized design of pelvic prostheses. Med Eng Phys. 2019;69:8–16.
33. Ün K, Çalık A. Relevance of inhomogeneous–anisotropic models of human cortical bone: a tibia study using the finite element method. Biotechnol Biotechnol Equip. 2016;30(3):538–47.
34. Saghaei Z, Hashemi A. Homogeneous material models can overestimate stresses in high tibial osteotomy: a finite element analysis. Proc Inst Mech Eng H. 2023;237(2):224–32.
35. Zhou R, Xue H, Wang J, Wang X, Wang Y, Zhang A, et al. Improving the stability of a hemipelvic prosthesis based on bone mineral density screw channel and prosthesis optimization design. Front Bioeng Biotechnol. 2022;10: 892385.
36. Moussa A, Rahman S, Xu M, Tanzer M, Pasini D. Topology optimization of 3D-printed structurally porous cage for acetabular reinforcement in total hip arthroplasty. J Mech Behav Biomed Mater. 2020;105: 103705.
37. Shi D, Wang F, Wang D, Li X, Wang Q. 3-D finite element analysis of the influence of synovial condition in sacroiliac joint on the load transmission in human pelvic system. Med Eng Phys. 2014;36(6):745–53.
38. Wong TM, Lau TW, Li X, Fang C, Yeung K, Leung F. Masquelet technique for treatment of posttraumatic bone defects. ScientificWorldJournal. 2014;2014: 710302.
39. Li Z, Lu M, Zhang Y, Wang J, Wang Y, Gong T, et al. Intercalary prosthetic reconstruction with three-dimensional-printed custom-made porous component for defects of long bones with short residual bone segments after tumor resection. Orthop Surg. 2024;16(2):374–82.
40. Wang H, Wan Y, Li Q, Xia Y, Liu X, Liu Z, et al. Porous fusion cage design via integrated global–local topology optimization and biomechanical analysis of performance. J Mech Behav Biomed Mater. 2020;112: 103982.
41. Peng MJ, Cao X, Chen HY, Hu Y, Li X, Lao Y, et al. Intralesional curettage versus prosthetic replacement for bone tumors—a finite element analysis case of limb salvage simulation in biomechanics. Comput Methods Programs Biomed. 2021;198: 105775.
42. Li Z, Kim JE, Davidson JS, Etheridge BS, Alonso JE, Eberhardt AW. Biomechanical response of the pubic symphysis in lateral pelvic impacts: a finite element study. J Biomech. 2007;40(12):2758–66.
43. Long M, Rack HJ. Titanium alloys in total joint replacement—a materials science perspective. Biomaterials. 1998;19(18):1621–39.
44. Dong E, Wang L, Iqbal T, Li D, Liu Y, He J, et al. Finite element analysis of the pelvis after customized prosthesis reconstruction. J Bionic Eng. 2018;15(3):443–51.
45. Wang Y, Chen W, Zhang L, Xiong C, Zhang X, Yu K, et al. Finite element analysis of proximal femur bionic nail (pfbn) compared with proximal femoral nail antirotation and intertan in treatment of intertrochanteric fractures. Orthop Surg. 2022;14(9):2245–55.
46. Guo Y, Guo W. Study and numerical analysis of Von Mises stress of a new tumor-type distal femoral prosthesis comprising a peek composite reinforced with carbon fibers: finite element analysis. Comput Methods Biomech Biomed Engin. 2022;25(15):1663–77.
47. Zhao Z, Yan T, Guo W, Yang R, Tang X. Is double-strut fibula ankle arthrodesis a reliable reconstruction for bone defect after distal tibia tumor resection? A finite element study based on promising clinical outcomes. J Orthop Surg Res. 2021;16(1):230.
48. Li X, Ji T, Huang S, Wang C, Zheng Y, Guo W. Biomechanics study of a 3D printed sacroiliac joint fixed modular hemipelvic endoprosthesis. Clin Biomech (Bristol, Avon). 2020;74:87–95.
49. Zhang Y, Min L, Lu M, Wang J, Wang Y, Luo Y, et al. Three-dimensional-printed customized prosthesis for pubic defect: prosthesis design and surgical techniques. J Orthop Surg Res. 2020;15(1):261.
50. Wang J, Min L, Lu M, Zhang Y, Wang Y, Luo Y, et al. What are the complications of three-dimensionally printed, custom-made, integrative hemipelvic endoprostheses in patients with primary malignancies involving the acetabulum, and what is the function of these patients? Clin Orthop Relat Res. 2020;478(11):2487–501.
51. Xu S, Guo Z, Shen Q, Peng Y, Li J, Li S, et al. Reconstruction of tumor-induced pelvic defects with customized, three-dimensional printed prostheses. Front Oncol. 2022;12: 935059.
52. Park JW, Kang HG, Kim JH, Kim HS. The application of 3D-printing technology in pelvic bone tumor surgery. J Orthop Sci. 2021;26(2):276–83.
53. Broekhuis D, Boyle R, Karunaratne S, Chua A, Stalley P. Custom designed and 3D-printed titanium pelvic implants for acetabular reconstruction after tumour resection. Hip Int. 2023;33(5):905–15.
54. Liu D, Jiang J, Wang L, Liu J, Jin Z, Gao L, et al. In vitro experimental and numerical study on biomechanics and stability of a novel adjustable hemipelvic prosthesis. J Mech Behav Biomed Mater. 2019;90:626–34.
55. Park JW, Shin YC, Kang HG, Park S, Seo E, Sung H, et al. In vivo analysis of post-joint-preserving surgery fracture of 3D-printed Ti–6Al–4V implant to treat bone cancer. Bio-Des Manuf. 2021;4(4):879–88.
56. Iqbal T, Shi L, Wang L, Liu Y, Li D, Qin M, et al. Development of finite element model for customized prostheses design for patient with pelvic bone tumor. Proc Inst Mech Eng H. 2017;231(6):525–33.
57. Hu X, Wen Y, Lu M, Luo Y, Zhou Y, Yang X, et al. Biomechanical and clinical outcomes of 3D-printed versus modular hemipelvic prostheses for limb-salvage reconstruction following periacetabular tumor resection: a mid-term retrospective cohort study. J Orthop Surg Res. 2024;19(1):258.

Publisher's Note